



Sulfhydration of AKT triggers Tau-phosphorylation by activating glycogen synthase kinase 3 β in Alzheimer's disease

Tanusree Sen^a, Pampa Saha^a, Tong Jiang^a, and Nilkantha Sen^{a,1}

^aDepartment of Neurological Surgery, University of Pittsburgh, Pittsburgh, PA 15213

Edited by Solomon H. Snyder, The Johns Hopkins University School of Medicine, Baltimore, MD, and approved January 21, 2020 (received for review September 27, 2019)

In Alzheimer's disease (AD), human Tau is phosphorylated at S199 (hTau-S199-P) by the protein kinase glycogen synthase kinase 3 β (GSK3 β). hTau-S199-P mislocalizes to dendritic spines, which induces synaptic dysfunction at the early stage of AD. The AKT kinase, once phosphorylated, inhibits GSK3 β by phosphorylating it at S9. In AD patients, the abundance of phosphorylated AKT with active GSK3 β implies that phosphorylated AKT was unable to inactivate GSK3 β . However, the underlying mechanism of the inability of phosphorylated AKT to phosphorylate GSK3 β remains unknown. Here, we show that total AKT and phosphorylated AKT was sulfhydrated at C77 due to the induction of intracellular hydrogen sulfide (H₂S). The increase in intracellular H₂S levels resulted from the induction of the proinflammatory cytokine, IL-1 β , which is a pathological hallmark of AD. Sulfhydrated AKT does not interact with GSK3 β , and therefore does not phosphorylate GSK3 β . Thus, active GSK3 β phosphorylates Tau aberrantly. In a transgenic knockin mouse (AKT-KI^{+/+}) that lacked sulfhydrated AKT, the interaction between AKT or phosphorylated AKT with GSK3 β was restored, and GSK3 β became phosphorylated. In AKT-KI^{+/+} mice, expressing the pathogenic human Tau mutant (hTau-P301L), the hTau S199 phosphorylation was ameliorated as GSK3 β phosphorylation was regained. This event leads to a decrease in dendritic spine loss by reducing dendritic localization of hTau-S199-P, which improves cognitive dysfunctions. Sulfhydration of AKT was detected in the postmortem brains from AD patients; thus, it represents a posttranslational modification of AKT, which primarily contributes to synaptic dysfunction in AD.

AKT | Tau phosphorylation | sulfhydration | GSK3 β

Alzheimer's disease (AD) is characterized by a progressive loss of memory, cognitive impairments, behavioral difficulties, and ultimately death (1–3). Synaptic dysfunction and hence memory impairments emerge early in the disease process (1, 4, 5). The microtubule-associated protein Tau is most abundant in the neuronal axons in healthy cells; however, at the early stages of AD, Tau can be mislocalized to dendrites after its specific phosphorylation at S199 (6–8). Human Tau (hTau) phosphorylation at S199 triggers synaptotoxicity independent of Tau aggregation and correlates with memory impairment in AD (9–11). Among the kinases that phosphorylate Tau, glycogen synthase kinase 3 β (GSK3 β) is implicated in AD pathology because activation of GSK3 β is essential for Tau phosphorylation at S199 (12–16). However, the molecular mechanism responsible for Tau phosphorylation at S199 remains poorly understood.

GSK3 β is a constitutively active kinase that is inactivated by phosphorylation at S9 (17, 18). In GSK3 β -S9A transgenic mice overexpressing hTau, Tau phosphorylation was increased (19). AKT is a serine/threonine kinase that phosphorylates GSK3 β at S9 (20, 21). Thus, AKT plays a critical role in the modulation of GSK3 β activity. Therefore, engagement of signaling pathways that activate AKT results in the phosphorylation of GSK3 β at S9, followed by down-regulation of GSK3 β activity (22). AKT is activated by phosphorylation at T308 and S473, which are located in the regulatory domain of the enzyme (20, 23). The brains of AD

patients contain highly abundant levels of active phosphorylated AKT (24, 25) concomitant with an increase in GSK3 β activity (26–28). However, it remains undetermined how GSK3 β remains activated even in the presence of phosphorylated AKT.

The early induction of inflammatory cytokines is the most common feature in vulnerable areas of AD patients' brains and body fluids (29–32). These inflammatory cytokines are associated with the cognitive decline observed in AD patients (33). Previously, we showed that the proinflammatory cytokine, IL-1 β , could induce intracellular hydrogen sulfide (H₂S) levels by augmenting the expression of cystathionine β -synthase (CBS), which catalyzes the formation of H₂S (34). H₂S is a gasotransmitter that activates intracellular signaling pathways through the sulfhydration of proteins. This modification occurs when the sulfur from H₂S attaches to a cysteine residue (–SH) of a protein and converts it to –SSH (35, 36).

In the present study, we show that sulfhydration of total or phosphorylated AKT inhibits its interaction with GSK3 β and subsequently down-regulates the phosphorylation and inactivation of GSK3 β . The activated GSK3 β facilitates Tau phosphorylation and cognitive dysfunction. In AKT knockin mice (AKT-KI^{+/+}), where the sulfhydration of AKT was blocked, early Tau phosphorylation at S199 was attenuated upon stimulation with the proinflammatory cytokine, IL-1 β .

Results

IL-1 β Induces H₂S-Dependent Tau Phosphorylation at S199. Tau can be mislocalized to dendrites after its specific phosphorylation at

Significance

It is well known that AKT inactivates glycogen synthase kinase 3 β (GSK3 β) by increasing its phosphorylation. The inactivation of GSK3 β leads to aberrant phosphorylation of Tau, which is a hallmark of Alzheimer's disease. However, we found that if phosphorylated AKT is sulfhydrated, it will be unable to inactivate GSK3 β and subsequently increases Tau phosphorylation. The influence of sulfhydrated AKT on GSK3 β and Tau phosphorylation was reversed in a transgenic AKT-KI^{+/+} mouse, where sulfhydration of AKT residue was mutated to alanine. Thus, AKT-sulfhydration represents a unique posttranslational modification of AKT that can be targeted to suppress phosphorylation of GSK3 β and subsequently reduce Tau phosphorylation.

Author contributions: T.S. and N.S. designed research; T.S., P.S., T.J., and N.S. performed research; T.S. and N.S. contributed new reagents/analytic tools; T.S. and N.S. analyzed data; and T.S. and N.S. wrote the paper.

The authors declare no competing interest.

This article is a PNAS Direct Submission.

Published under the PNAS license.

¹To whom correspondence may be addressed. Email: SENN@pitt.edu.

This article contains supporting information online at <https://www.pnas.org/lookup/suppl/doi:10.1073/pnas.1916895117/-DCSupplemental>.

First published February 12, 2020.

S199 (6–8). Therefore, we monitored the phosphorylation of Tau at S199 in AD patients' brains and a mouse model of AD (PS19). PS19 mice contain the hTau mutant (hTau-P301S) that is characterized by impaired synaptic function before fibrillary Tau tangles emerge at the age of 6 to 8 mo (37). We found that Tau phosphorylation at S199 was abundant in both AD patients' brains (Fig. 1A and *SI Appendix, Fig. S1A*) and in the cortex and hippocampus of PS19 mice within the age of 2 mo (Fig. 1B and *SI Appendix, Fig. S1B*). Since IL-1 β is highly abundant in AD patients' brains and body fluids (38), and is associated with cognitive decline (33), we monitored the mRNA and protein levels of IL-1 β in both the cortex and hippocampus of PS19 mice. We found that both IL-1 β mRNA (Fig. 1C) and protein levels (Fig. 1D) were significantly increased in PS19 mice that were 2-month-old. These data suggest that inflammation in PS19 mice is associated with Tau phosphorylation. However, in order to determine whether IL-1 β is directly responsible for Tau phosphorylation, we overexpressed hTau-P301L in primary neurons before treatment with IL-1 β . We found that IL-1 β induced a robust increase in hTau phosphorylation at S199 (Fig. 1E and *SI Appendix, Fig. S1C*).

These data suggest that IL-1 β is directly responsible for hTau phosphorylation. Thus, we explored the underlying mechanism of how IL-1 β induces Tau phosphorylation at S199.

Previously, we showed that IL-1 β could induce the expression of CBS, a catalytic enzyme responsible for synthesizing H₂S (34). Thus, we hypothesized that IL-1 β induces hTau phosphorylation by a mechanism that is dependent on H₂S. In order to test this hypothesis, we monitored the intracellular levels of both CBS and H₂S in murine PS19 brains. Consistent with our previous publication (34), we found that the expression of CBS (Fig. 1F and G and *SI Appendix, Fig. S1D and E*) and intracellular H₂S (Fig. 1H and I and *SI Appendix, Fig. S1F and G*) was increased in the cortex and hippocampus of PS19 mice. Furthermore, we found that the depletion of CBS (CBS RNAi) markedly reduced Tau phosphorylation at S199 in the cortex after administration of IL-1 β to PS19 mice, as monitored by Western blotting (Fig. 1J and *SI Appendix, Fig. S1H*) and confocal analyses (Fig. 1K and *SI Appendix, Fig. S1I*). These data indicate that H₂S plays an essential role in facilitating Tau phosphorylation. To further confirm our cell culture data in mice, we administered IL-1 β to

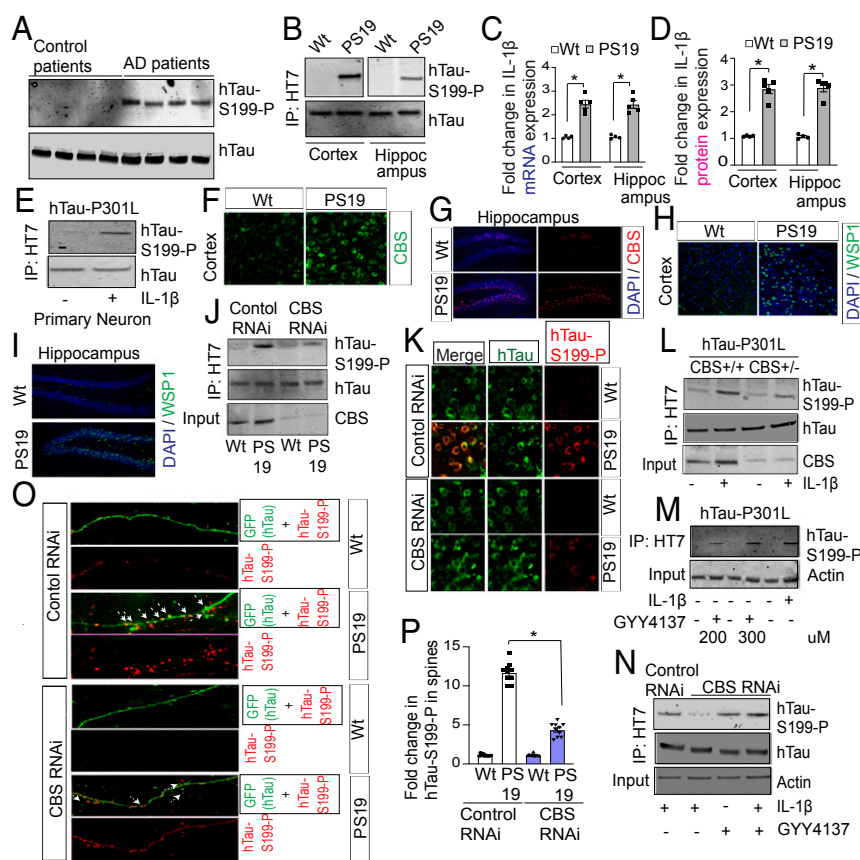


Fig. 1. IL-1 β induces Tau-phosphorylation in an H₂S-dependent manner. (A) Western blot analysis using brain extracts isolated from AD patients and age-matched control brains showed that hTau-S199P level was increased. (B) Immunoprecipitation analysis using HT7 antibody explains that hTau-S199 phosphorylation (hTau-S199P) was increased in the cortex and hippocampus of PS19 mice. (C and D) The mRNA level of IL-1 β measured by quantitative RT-PCR and protein level of IL-1 β by ELISA were increased in the cortex and hippocampus of PS19 mice. (E) Administration of IL-1 β induces hTau-S199 phosphorylation in primary neurons overexpressing hTau-P301L. (F and G) The immunofluorescent staining shows that the expression level of CBS was increased in the cortex (F) and hippocampus (G) of PS19 mice. (H and I) Intracellular H₂S level (WSP1; green fluorescence) was increased in the cortex (H) and hippocampus (I) of PS19 mice. (J) The depletion of CBS by administration of CBS RNAi reduces hTau-S199 phosphorylation in the cortex of PS19 mice. (K) Confocal analysis showed that depletion of CBS by CBS RNAi reduces hTau-S199 phosphorylation in the cortex of PS19 mice. (L) The hTau-S199 phosphorylation was reduced in primary neurons isolated from CBS^{+/-} mice compared to CBS^{+/+} neurons overexpressed with hTau-P301L and treated with IL-1 β (10 ng/mL) for 24 h. (M) The phosphorylation of hTau-S199 was increased in primary neurons overexpressing hTau-P301L after administration of IL-1 β or GYY4137 (200, 300 μ M). (N) administration of GYY4137 (300 μ M) with or without IL-1 β increases hTau-S199P in primary neurons depleted with CBS. (O and P) Confocal microscopic analysis (O) and quantitative analysis (P) using ImageJ showed that localization of hTau-S199P in dendrites were decreased in dendritic spines in PS19 mice after depletion of CBS. One-way ANOVA measured statistical significance with a Tukey-Kramer post hoc correction, $n = 7$, $*P < 0.05$. All data are expressed as mean \pm SEM. The arrowheads in O indicate the dendritic spines. (Magnification: G-I, 20 \times ; K, 40 \times ; O, 60 \times .)

CBS^{+/+} and CBS^{+/-} mice overexpressing hTau-P301L in the cortex. In the PS19 brain, aberrant activation of nonneuronal cells, such as microglial cells, mostly contribute to the increase in IL-1 β in the brain (37, 39). However, the production of inflammatory molecules in a healthy brain is minimal. Thus, to mimic the pathological conditions that are present in the PS19 brain, we administered IL-1 β to CBS^{+/+} and CBS^{+/-} mice overexpressing hTau-P301L in the cortex. This study revealed that Tau phosphorylation was significantly decreased in CBS^{+/-} mice compared to CBS^{+/+} mice (Fig. 1L and *SI Appendix, Fig. S1J*), but we could still detect Tau phosphorylation in the CBS^{+/-} mice. This may be explained by the fact that the intracellular H₂S levels were significantly decreased in CBS^{+/-} mice, but not fully eliminated.

In order to directly monitor the influence of H₂S on hTau phosphorylation, we administered the H₂S donor, GYY4137, to primary neurons overexpressing hTau-P301L. We found that GYY4137 induced Tau phosphorylation at S199 in a dose-dependent manner. Furthermore, the increase in GYY4137-induced hTau phosphorylation was comparable to the hTau phosphorylation levels observed when IL-1 β was administered to primary neurons overexpressing hTau-P301L (Fig. 1M and *SI Appendix, Fig. S1K*). We also found that administration of GYY4137 induced hTau phosphorylation in CBS-depleted neurons, and the increase in hTau phosphorylation was not further elevated after administration of IL-1 β (Fig. 1N and *SI Appendix, Fig. S1L*). These data suggest that H₂S, generated by CBS, is critical for IL-1 β -induced phosphorylation of hTau at S199.

Since phosphorylation of Tau at S199 leads to its mislocalization to the spines (6–8), we monitored the localization of phosphorylated Tau in the spines of primary neurons isolated from PS19 mice. We found that phosphorylated Tau was highly abundant in the spines; however, it was reduced in CBS-depleted neurons (Fig. 1O and P). These data suggest that H₂S plays an essential role in

regulating Tau phosphorylation, and the mislocalization of phosphorylated Tau to dendrites is induced by inflammatory stimuli. However, the underlying mechanism of how H₂S induces hTau phosphorylation at S199 remains unanswered.

H₂S Down-Regulates GSK3 β Phosphorylation without Affecting AKT Phosphorylation. Previous reports have suggested that the activation of protein kinase GSK3 β is essential for Tau phosphorylation at S199 and GSK3 β activity is inhibited by phosphorylation at S9 (17, 18). A decrease in GSK3 β phosphorylation due to the inactivation of another protein kinase, AKT, leads to GSK3 β activation (17, 21). The phosphorylation of T308 and S473 is necessary for the activation of AKT (40, 41). We monitored the phosphorylation levels of AKT and GSK3 β in AD patients' brains as well as the cortex and hippocampus of PS19 mice. Consistent with previous data (42), we found that AKT remained phosphorylated at S473 and T308 in AD patients' brains (Fig. 2A and *SI Appendix, Fig. S2A*) as well as the cortex and hippocampus of PS19 mice (Fig. 2B and *SI Appendix, Fig. S2B and C*). However, the phosphorylation of GSK3 β at S9 was decreased in the AD patients' brains (Fig. 2A and *SI Appendix, Fig. S2A*), as well as the cortex and hippocampus of PS19 mice (Fig. 2B and *SI Appendix, Fig. S2B and C*). To further confirm these results, we administered IL-1 β to primary neurons isolated from CBS^{+/-} mice overexpressing hTau-P301L. Consistent with our *in vivo* results, we found that IL-1 β did not affect AKT phosphorylation but reduced GSK3 β phosphorylation at S9 (Fig. 2C and *SI Appendix, Fig. S2D*). Furthermore, we observed that depletion of CBS in the PS19 cortex increased GSK3 β phosphorylation at S9 without affecting the AKT phosphorylation status (Fig. 2D and *SI Appendix, Fig. S2E*). These data suggest that H₂S plays a significant role in regulating GSK3 β phosphorylation, but it does not affect AKT phosphorylation. Since AKT is the major kinase

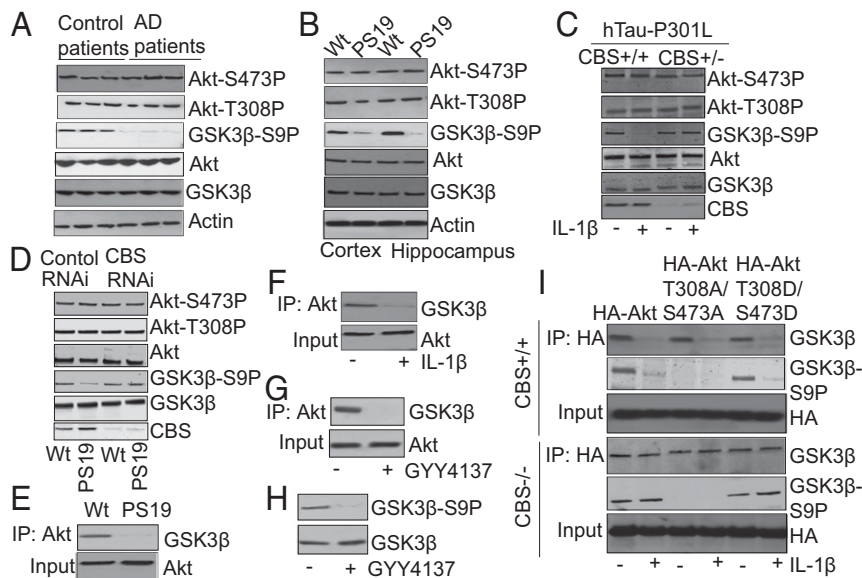


Fig. 2. Phosphorylation of GSK3 β is dependent on H₂S. (A) Western blot analysis using brain tissue lysates of AD patients showed that AKT phosphorylation at S473 (AKT-S473P) and T308 (AKT-T308P) remains unaltered, but phosphorylation of GSK3 β at S9 (GSK3 β S9P) was decreased significantly. (B) Phosphorylation of AKT at S473 (AKT-S473P) and T308 (AKT-T308P) remains unaltered but phosphorylation of GSK3 β at S9 (GSK3 β S9P) was decreased in the cortex and hippocampus of PS19 mice analyzed by Western blot. (C) Administration of IL-1 β in CBS^{+/-} mice overexpressing hTau-P301L rescued phosphorylation of GSK3 β at S9 (GSK3 β S9P) compared to CBS^{+/+} mice overexpressing hTau-P301L. (D) Western blot analysis showed that depletion of CBS after administration of CBS RNAi in PS19 mice rescued phosphorylation of GSK3 β at S9 (GSK3 β S9P) although AKT phosphorylation at S473 (AKT-S473P) and T308 (AKT-T308P) remained unaltered. (E) The interaction between AKT and GSK3 β was decreased in PS19 mice and analyzed by coimmunoprecipitation (co-IP) analysis. (F) Administration of IL1 β (10 ng) causes a decrease in the interaction between AKT and GSK3 β in primary neuron culture. (G and H) Administration of GYY4137 (300 μ M) causes a decrease in the interaction between AKT and GSK3 β and the phosphorylation of GSK3 β at S9 residue. (I) CBS^{+/+} or CBS^{-/-} neurons overexpressing HA-AKT, HA-AKT-T308A/S473A, or HA-AKT-T308D/S473D were treated with IL-1 β . Administration of IL-1 β affects interaction between Akt and GSK3 β and phosphorylation of GSK3 β in CBS^{+/+} neurons compared to CBS^{-/-} neurons.

that phosphorylates GSK3 β , we investigated the mechanism of how H₂S regulates GSK3 β phosphorylation without affecting AKT phosphorylation.

In order to determine whether the phosphorylation status of GSK3 β is dependent on the AKT–GSK3 β complex, we monitored the interaction between AKT and GSK3 β by coimmunoprecipitation assays using cortical lysates from PS19 mice. We found that the interaction between AKT and GSK3 β was reduced in cortical lysates from PS19 mice compared to wild-type mice (Fig. 2E and *SI Appendix, Fig. S2F*). These results were further confirmed in primary neurons treated with IL-1 β , which also had significantly reduced levels of the AKT–GSK3 β complex compared to untreated cells (Fig. 2F and *SI Appendix, Fig. S2G*). In order to study the effects of GYY4137 on the interaction between AKT and GSK3 β , as well as the phosphorylation of GSK3 β , we treated primary neurons with GYY4137. We found that GYY4137-treated cells had decreased levels of the AKT–GSK3 β complex (Fig. 2G and *SI Appendix, Fig. S2H*), along with a reduction in GSK3 β phosphorylation (Fig. 2H and *SI Appendix, Fig. S2I*) compared to untreated cells. These data suggest that H₂S directly influences GSK3 β phosphorylation by modulating the AKT–GSK3 β interaction.

In order to elucidate whether the AKT–GSK3 β interaction is dependent on AKT phosphorylation, we generated the following constructs expressing either: 1) Wild-type AKT (HA-AKT), 2) a mutant of AKT that abolishes the phosphorylation of the amino acids which are required for AKT activation (phospho-mutant; HA-AKT-T308A/S473A), or 3) a phospho-mimic AKT mutant (HA-AKT-T308D/S473D). These constructs were overexpressed in CBS^{+/+} and CBS^{-/-} neurons and treated with IL-1 β . We found that the interaction between AKT and GSK3 β was decreased in neurons isolated from CBS^{+/+} mice following IL-1 β administration, irrespective of the overexpression of either the phospho-mutant or the phospho-mimic mutant of AKT (Fig. 2I and *SI Appendix, Fig. S2J*). However, in CBS-depleted cells, the interaction between AKT and GSK3 β remained unaltered with or without IL-1 β treatment. In addition, the interaction between AKT and GSK3 β remained unaltered after the overexpression of either the phospho-mutant or phospho-mimic mutant of AKT (Fig. 2I and *SI Appendix, Fig. S2J*). These data suggest that the interaction between AKT and GSK3 β is not dependent on AKT phosphorylation; however, intracellular H₂S levels, which were abolished in CBS^{-/-} neurons, can modulate the interaction between AKT and GSK3 β .

In order to examine whether the AKT–GSK3 β complex has any influence on GSK3 β phosphorylation, we monitored the phosphorylation of GSK3 β at S9 in IL-1 β -treated cells overexpressing HA-AKT, HA-AKT-T308A/S473A, or HA-AKT-T308D/S473D. We found lower levels of GSK3 β phosphorylation at S9 in cells where the interaction of HA-AKT or HA-AKT-T308D/S473D with GSK3 β was decreased after IL-1 β treatment (Fig. 2I and *SI Appendix, Fig. S2K*). Since HA-AKT-T308A/S473A is a dead-kinase mutant of AKT, we found that it was unable to phosphorylate GSK3 β irrespective of its interaction with GSK3 β with or without IL-1 β treatment (Fig. 2I and *SI Appendix, Fig. S2K*). These data suggest that the interaction between AKT and GSK3 β is independent of the phosphorylation status of AKT, but it is required for AKT to phosphorylate GSK3 β . Furthermore, we found that the phosphorylation of GSK3 β at S9 remained unaltered in cells overexpressed with HA-AKT-T308D/S473D with or without administration of IL-1 β (Fig. 2I and *SI Appendix, Fig. S2K*). These data suggest that phosphorylation of GSK3 β is dependent on the interaction between AKT and GSK3 β and intracellular H₂S levels is critical to regulate the AKT–GSK3 β interaction. However, the underlying mechanism of how H₂S regulates the interaction between AKT–GSK3 β has not been elucidated yet.

Sulfhydrylation of Phosphorylated AKT at C77 Inhibits the Formation of the AKT–GSK3 β Complex and Prevents the Phosphorylation of GSK3 β at S9. H₂S is known to function as an intracellular signaling molecule through the sulfhydrylation of proteins. Protein sulfhydrylation occurs when H₂S attaches to a cysteine residue in a protein and converts the –SH to an –SSH (35, 36). We tested whether AKT, phosphorylated AKT, or GSK3 β can be sulfhydrated in human AD samples. We detected sulfhydrated wild-type AKT (AKT-SSH) and sulfhydrated phosphorylated AKT (AKT-P-SSH) at either S473 (AKT-S473P-SSH) or T308 (AKT-T308P-SSH). However, GSK3 β was not sulfhydrated in AD patients' brains (Fig. 3A and *SI Appendix, Fig. S3A*). This was further confirmed in another experiment where administration of GYY4137 sulfhydrated HA-AKT-T308A/S473A, and HA-AKT-T308D/S473D to a similar extent as observed in neurons overexpressed with HA-AKT (Fig. 3B and *SI Appendix, Fig. S3B*). These data suggest that both wild-type AKT and the phosphorylated AKT can be sulfhydrated.

To further confirm these results, we analyzed the presence of AKT-SSH and AKT-P-SSH in the cortex and hippocampus of PS19 mice. We found that the levels of AKT-SSH, AKT-S473P-SSH, and AKT-T308P-SSH were highly abundant in the cortex and hippocampus of PS19 mice (Fig. 3C and *SI Appendix, Fig. S3C*). To determine the role of CBS and H₂S in AKT sulfhydrylation, we depleted CBS and monitored AKT sulfhydrylation in PS19 mice. Consistent with our previous results, we found that AKT-SSH, AKT-S473P-SSH, and AKT-T308P-SSH were decreased in CBS-depleted PS19 mice (Fig. 3D and *SI Appendix, Fig. S3D*). Consistent with these data, we found that depletion of CBS by RNAi in IL-1 β -treated primary neurons abolished the formation of AKT-SSH, AKT-S473P-SSH, and AKT-T308P-SSH (Fig. 3E and *SI Appendix, Fig. S3E*). However, overexpression of hTau-P301L did not affect AKT sulfhydrylation in IL-1 β -treated primary neurons (Fig. 3F and *SI Appendix, Fig. S3F*). This result suggests that hTau has no influence on the formation of AKT-S473P-SSH and AKT-T308P-SSH in a feed-forward mechanism.

In order to identify the Cys (C) residue responsible for AKT-SSH, we mutated four Cys residues within AKT and found that mutation of the C77 residue (Fig. 3G) to alanine (C77A) abolished the formation of AKT-SSH in HEK293 cells treated with GYY4137 (Fig. 3H and *SI Appendix, Fig. S3G*). The formation of AKT-SSH was further confirmed by the red maleimide assay. In this assay, Alexa Fluor 680 is conjugated to C2 maleimide (red maleimide), which selectively interacts with sulfhydryl groups of cysteines (Cs), thus labeling both sulfhydrated as well as unsulfhydrated Cs. However, treatment with DTT cleaves disulfide bonds, and thus the red signal from a sulfhydrated protein will be detached, but the red signal will be maintained on an unsulfhydrated protein. Thus, DTT treatment will result in decreased fluorescence of sulfhydrated proteins. The levels of protein sulfhydrylation were calculated as the residual red fluorescence intensity after DTT treatment divided by the total AKT level.

We employed the red maleimide assay in cells overexpressing either HA-AKT or HA-AKT-C77A. In cells overexpressing HA-AKT, we detected an intense red signal, which represented proteins with –SH as well as –SSH substituents. The intensity of this signal was reduced by >95% following DTT treatment, which indicated that HA-AKT was robustly sulfhydrated. In contrast, in cells overexpressing HA-AKT-C77A, no reduction in the red signal intensity was observed after DTT treatment, establishing that the putative sulfhydrylation of AKT was abolished by the C77A mutation (Fig. 3I and *SI Appendix, Fig. S3H*).

Similarly, overexpression of HA-AKT-C77A in IL-1 β -treated primary neurons blocked the formation of AKT-SSH, AKT-S473P-SSH, and AKT-T308P-SSH (Fig. 3I and *SI Appendix, Fig. S3I*), as detected by the modified biotin switch assay. Interestingly, the phosphorylation of AKT was not affected by mutating the C77

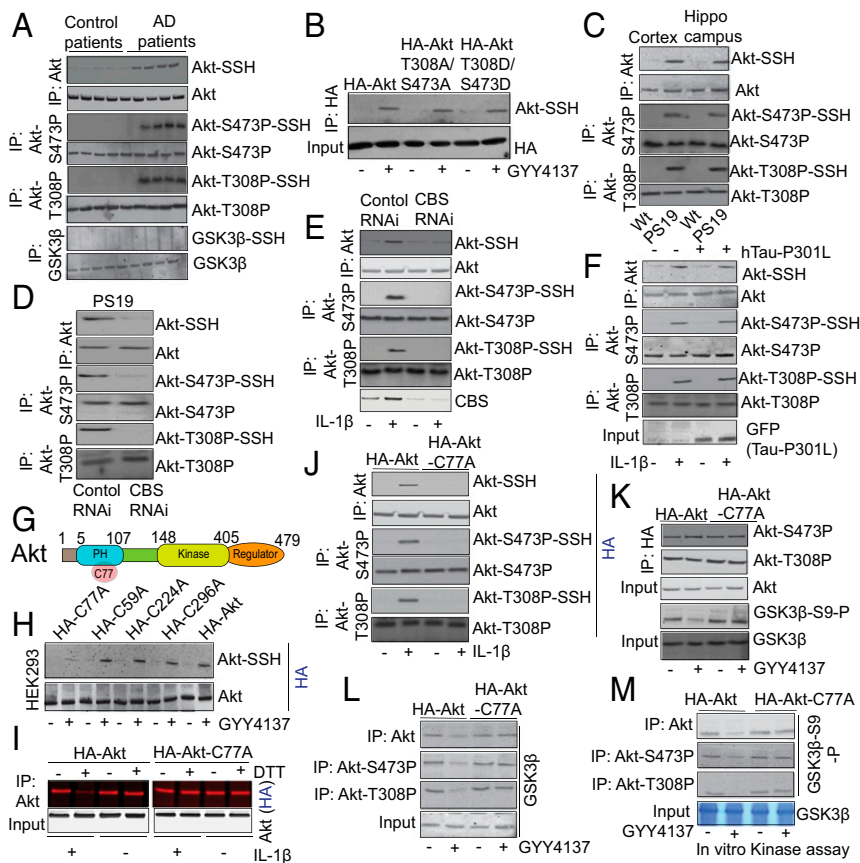


Fig. 3. Sulphydration of total or phosphorylated AKT regulates phosphorylation of GSK3 β at S9 residue. (A) The modified biotin assay detects sulphydration of total AKT (AKT-SSH) or phosphorylated AKT at S473 (AKT-S473P-SSH) or T308 (AKT-T308P-SSH) in the brain lysates of AD patients compared to age-matched control brains. However, GSK3 β was not sulphydrated in the AD patients. (B) Administration of GYY4137 (300 μ M) in primary neurons induces sulphydration of HA-AKT-S473A and HA-AKT-T308D/S473D. (C) Sulphydration of total AKT (AKT-SSH) or phosphorylated AKT at S473 (AKT-S473P-SSH) or T308 (AKT-T308P-SSH) were found in the cortex and hippocampus of PS19 mice by modified biotin switch assay. (D) Depletion of CBS after administration of CBS RNAi in PS19 mice blocks sulphydration of total AKT (AKT-SSH) or phosphorylated AKT at S473 (AKT-S473P-SSH) or T308 (AKT-T308P-SSH). (E) Depletion of CBS after administration of CBS RNAi blocks sulphydration of total AKT (AKT-SSH) or phosphorylated AKT at S473 (AKT-S473P-SSH) or T308 (AKT-T308P-SSH) in primary neurons treated with IL-1 β (10 ng/mL). (F) Overexpression of hTau-P301L did not affect sulphydration of total AKT (AKT-SSH) or phosphorylated AKT at S473 (AKT-S473P-SSH) or T308 (AKT-T308P-SSH) after administration of IL-1 β in primary neurons. (G) The schematic view shows that C77 resides within the PH domain of AKT which ranges from 5 to 107 amino acids. (H) The C59, C77A, C224, and C298A residues of AKT were mutated to alanine by site-directed mutagenesis. The HA-tagged mutants of AKT C59A, C77A, C224A, and C298A mutants were overexpressed in HEK293 cells and treated with GYY4137 (300 μ M) and subjected to modified biotin switch assay. All of the AKT-mutants except for AKT C77 were sulphydrated like wild-type AKT. (I) The red-maleimide assay (another method to detect sulphydration of proteins) shows that AKT can be sulphydrated at C77 residue in primary neurons treated with IL-1 β . (J) The induction of AKT-SSH, AKT-S473P-SSH, and AKT-T308P-SSH was abolished in primary neurons overexpressed with HA-AKT-C77A and treated with IL-1 β for 24 h. However, phosphorylation of AKT at S473 (AKT-S473P) or T308 (AKT-T308P) remains unaltered in cells overexpressed with either wild-type HA-AKT or HA-AKT-C77A mutant. (K) Overexpression of HA-AKT-C77A does not affect phosphorylation of AKT either at S473 (AKT-S473P) or T308 (AKT-T308P) but reduces phosphorylation of GSK3 β at S9 (GSK3 β -S9-P) in HEK293 cells. (L) Overexpression of AKT-C77A rescues the interaction between AKT, AKT-S473P, or AKT-T308P and GSK3 β after administration of GYY4137 (300 μ M) in HEK293 cells. (M) In vitro kinase assay showed that AKT, AKT-S473P, or AKT-T308P immunoprecipitated from GYY4137-treated HEK293 cells was unable to phosphorylate GSK3 β at S9 (GSK3 β -S9-P); however, the phosphorylation of GSK3 β at S9 (GSK3 β -S9-P) was rescued after overexpression of AKT-C77A mutant in HEK293 cells.

residue of AKT (Fig. 3J), which suggested that sulphydration is downstream of AKT phosphorylation. Similarly, we found that HA-AKT-C77A was phosphorylated to a similar extent as wild type AKT in GYY4137-treated HEK293 cells overexpressed with HA-AKT or HA-AKT-C77A (Fig. 3K and *SI Appendix, Fig. S3J*). However, overexpression of HA-AKT-C77A restores GSK3 β phosphorylation compared to cells overexpressing wild type HA-AKT after treatment with GYY4137. These data suggest that sulphydration does not directly influence AKT phosphorylation at S473 and T308.

In order to understand whether the sulphydration of phosphorylated AKT has any influence on the interaction between GSK3 β and AKT, we overexpressed HA-AKT or HA-AKT-C77A in GYY4137-treated HEK293 cells. We found that in HA-AKT-

C77A-overexpressing cells, the interaction between phosphorylated AKT and GSK3 β was detected along with an increase in the phosphorylation of GSK3 β at S9 after treatment with GYY4137 (Fig. 3L and *SI Appendix, Fig. S3K*). These data suggest that sulphydration of AKT blocks its interaction with GSK3 β and subsequently affects the phosphorylation of GSK3 β .

This was further confirmed by an in situ kinase activity assay. In this assay, both wild-type HA-AKT and the HA-AKT-C77A mutant were overexpressed in GYY4137-treated HEK293 cells, and AKT or phosphorylated AKT was immunoprecipitated from the cells followed by a kinase activity assay using GSK3 β as the substrate. We found that phosphorylated AKT from HA-AKT-overexpressed untreated cells robustly phosphorylated GSK3 β . However, phosphorylated AKT immunoprecipitated from

AKT-C77A-overexpressing cells phosphorylated GSK3 β irrespective of GYY4137 treatment (Fig. 3M and *SI Appendix, Fig. S3L*). These data confirm that sulfhydrylation of AKT phosphorylated at either S473 or T308 is a key posttranslational modification that reduces the phosphorylation of GSK3 β in an H₂S-dependent manner.

AKT Sulfhydrylation Was Abolished and GSK3 β Phosphorylation Was Restored in a Transgenic AKT Knockin Mouse (AKT-KI^{+/+}). In order to determine whether AKT-C77A has any influence on the kinase activity of GSK3 β in vivo, we generated a knockin mouse containing a mutated C77 residue in AKT that was substituted with alanine (AKT-C77A) using a modified version of the CRISPR-Cas9 technology (*SI Appendix, Fig. S4A*). The generation of AKT-KI^{-/-}, AKT-KI^{-/+}, and AKT-KI^{+/+} mice was confirmed by genotyping (Fig. 4A). There were no gross differences between the AKT-KI^{-/-} and AKT-KI^{+/+} mice either from the dorsal, ventral, or lateral view, as well as brain size (Fig. 4B). The bodyweight of the AKT-KI^{+/+} mice increased with their age irrespective of the gender, and the increase was comparable to the AKT-KI^{-/-} mice (Fig. 4C). In order to more fully examine the knockin mice, we analyzed the brain sections of AKT-KI^{-/-} and AKT-KI^{+/+} mice. We did not observe any remarkable differences in the cellular morphology or in the total number of cells in the brain sections of

the cortex and hippocampus of AKT-KI^{-/-} and AKT-KI^{+/+} mice (Fig. 4D). In addition, there was no difference in the movement time and in the percentage of time spent in the center during the open-field test of AKT-KI^{-/-} and AKT-KI^{+/+} mice (Fig. 4E and F). These data suggest that there is no difference in locomotor activity between AKT-KI^{-/-} and AKT-KI^{+/+} mice at the physiological level.

In order to determine whether AKT sulfhydrylation can be blocked in AKT-KI^{+/+} mice, we administered IL-1 β to these mice. IL-1 β induction does not occur in either AKT-KI^{+/+} or AKT-KI^{-/-} mice under physiological conditions. Thus, to mimic the inflammatory state, we administered IL-1 β to the mice. We found that administration of IL-1 β to AKT-KI^{+/+} mice prevented the formation of AKT-SSH, AKT-S473P-SSH, and AKT-T308P-SSH in the cortex and hippocampus. However, AKT was not sulfhydrylated at the physiological level in the absence of IL-1 β treatment (Fig. 4G and *SI Appendix, Fig. S4B*). Similarly, we found that in primary neurons isolated from AKT-KI^{+/+} mice, the formation of AKT-SSH, AKT-S473P-SSH, and AKT-T308P-SSH was abolished after administration of either IL-1 β or GYY4137 compared to AKT-KI^{-/-} mice. However, the phosphorylation of AKT at either S473 (AKT-S473P) or T308 (AKT-T308P) remained unaltered in murine AKT-KI^{+/+} neurons compared to

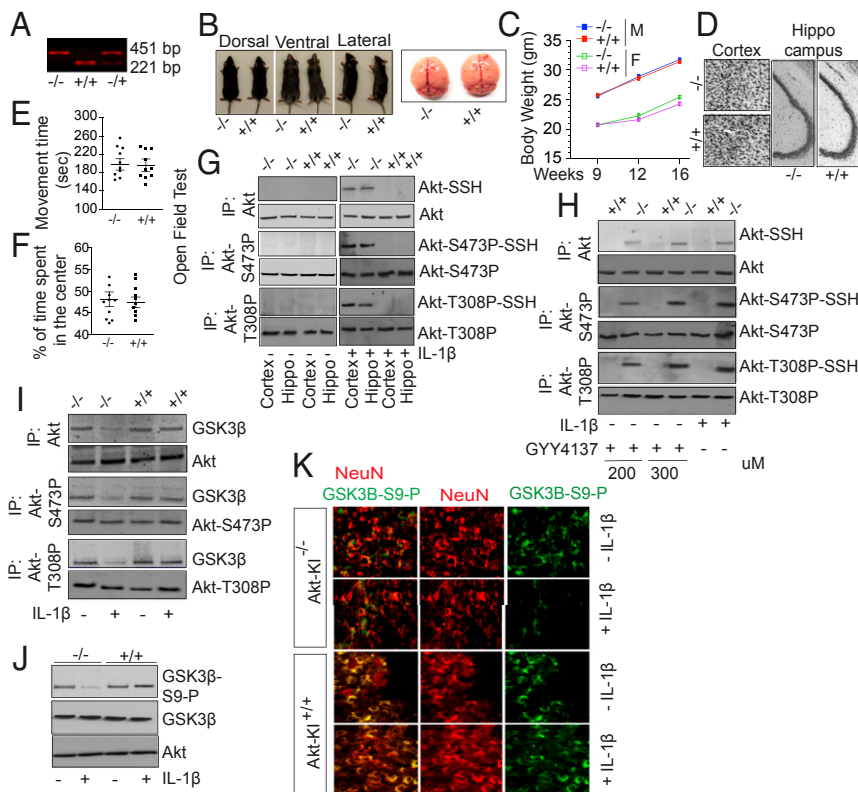


Fig. 4. In AKT-KI^{+/+} mice, sulfhydrylation of AKT was prevented, and phosphorylation of GSK3 β at S9 was rescued along with an increase in interaction between AKT and GSK3 β . (A) The representative DNA electrophoresis image of Sac-I digester PCR product from genomic DNA showing genotypic profile of $-/-$ (wild-type), $-/+$ (heterozygous), and $+/+$ (knockin) mice. (B) The dorsal view, ventral view, and lateral view of wild-type and AKT-KI 10-wk-old adult mice and the brain images. (C) The bodyweight of AKT-KI^{-/-} and AKT-KI^{+/+} mice from 9 to 16 wk of age. (D) The Cresyl violet staining of cortex and hippocampus of adult 12-wk-old AKT-KI^{-/-} and AKT-KI^{+/+} mice. (E and F) The total movement time (E) and percentage of time spent in the center (F) remain unaltered in AKT-KI^{-/-} and AKT-KI^{+/+} mice. One-way ANOVA measured statistical significance with a Tukey-Kramer post hoc correction, $n = 10$, $*P < 0.05$. All data are expressed as mean \pm SEM. (G) Sulfhydrylation of total AKT (AKT-SSH) or phosphorylated AKT at S473 (AKT-S473P-SSH) or T308 (AKT-T308P-SSH) was blocked in the cortex and hippocampus of AKT-KI^{+/+} mice after administration of IL-1 β . (H) Primary neurons isolated from AKT-KI^{+/+} mice were unable to sulfhydrylate total AKT (AKT-SSH) or phosphorylated AKT at S473 (AKT-S473P-SSH) or T308 (AKT-T308P-SSH) after administration of IL-1 β (10 ng) or GYY4137 (300 μ M). (I) The interaction between total AKT, AKT-S473P, or AKT-T308P and GSK3 β was restored in AKT-KI^{+/+} mice compared to AKT-KI^{-/-} mice after administration of IL-1 β in the cortex. (J) The reduction of GSK3 β -S9-P was rescued after administration of IL-1 β in the cortex of AKT-KI^{+/+} mice and it was measured by Western blot analysis. (K) The confocal analysis shows that GSK3 β -S9-P was decreased in the cortex of IL-1 β -treated AKT-KI^{-/-} mice and it was rescued in IL-1 β -treated AKT-KI^{+/+} mice. One-way ANOVA measured statistical significance with a Tukey-Kramer post hoc correction, $n = 7$, $*P < 0.05$. All data are expressed as mean \pm SEM. (Magnification: D, 20 \times ; K, 40 \times .)

murine AKT-KI^{-/-} neurons (Fig. 4H and *SI Appendix, Fig. S4C*). These data suggest that IL-1 β induced the formation of AKT-SSH, AKT-S473P-SSH, and AKT-T308P-SSH by elevating intracellular H₂S levels. However, the formation of AKT-SSH, AKT-S473P-SSH, and AKT-T308P-SSH can be blocked in AKT-KI^{+/+} mice.

Our data show that a reduction in AKT-SSH, AKT-S473P-SSH, or AKT-T308P-SSH rescued the interaction between GSK3 β and AKT, AKT-S473P, or AKT-T308P in AKT-KI^{+/+} mice compared to AKT-KI^{-/-} mice after treatment with IL-1 β (Fig. 4I and *SI Appendix, Fig. S4D*). An increased interaction between phosphorylated AKT and GSK3 β restored GSK3 β phosphorylation at S9 in AKT-KI^{+/+} mice compared to AKT-KI^{-/-} mice after administration of IL-1 β (Fig. 4J and *SI Appendix, Fig. S4E*). This was further confirmed by confocal microscopy analysis, where the reduction in GSK3 β phosphorylation at S9 was restored in AKT-KI^{+/+} mice following administration of IL-1 β (Fig. 4K and *SI Appendix, Fig. S4F*). Taken together, our data show that GSK3 β phosphorylation at S9 was restored in AKT-KI^{+/+} mice after IL-1 β administration. Thus, it is important to understand whether blocking the formation of AKT-SSH in the PS19 brain can reduce Tau phosphorylation.

IL-1 β -Treated AKT-KI^{+/+} Mice Overexpressing hTau-P301L Have Reduced hTau Phosphorylation Levels That Prevent the Loss of Dendritic Spines and Improve Memory Functions. We attempted to generate a homozygous PS19^{+/+}:Akt-KI^{+/+} mice colony to test the influence of AKT-SSH on Tau phosphorylation in PS19 mice. Unfortunately, we found that establishing a homozygous PS19^{+/+}:AKT-KI^{+/+} mice colony was unfeasible because female PS19^{+/+}:AKT-KI^{+/+} mice were infertile like the female PS19^{+/+} mice. However, we studied heterozygous PS19^{+/+}:Akt-KI^{+/+} mice to elucidate the role of AKT sulphydration in Tau phosphorylation. We found that Tau phosphorylation was reduced in PS19^{+/+}:Akt-KI^{+/+} mice compared to PS19^{+/+}:Akt-KI^{-/-} mice (*SI Appendix, Fig. S5A*) and the PS19^{+/+}:Akt-KI^{+/+} mice showed improvement in spatial memory functions, which was determined by a Y-maze study. In this test, the total number of arm entries (*SI Appendix, Fig. S5A*), total alternations, and the number of total triad alternations are calculated. The total number of arm entries (*SI Appendix, Fig. S5B*) and total alternations (*SI Appendix, Fig. S5C*) are almost similar between PS19^{+/+}:Akt-KI^{-/-} mice and PS19^{+/+}:Akt-KI^{+/+} mice. This indicates that there were no major differences in motor functions of AKT-KI^{+/+} and AKT-KI^{-/-} mice. However, total triad alternations (*SI Appendix, Fig. S5D*) in the Y-maze was significantly reduced in PS19^{+/+}:Akt-KI^{-/-} mice compared to PS19^{+/+}:Akt-KI^{+/+} mice. These data suggest that blocking AKT sulphydration improved memory functions in PS19 mice.

These encouraging data prompted us to determine whether homozygous AKT-KI^{+/+} mice fully block Tau phosphorylation and restore cognitive functions. To test this hypothesis, we overexpressed hTau-P301L in the brains of both AKT-KI^{-/-} and AKT-KI^{+/+} mice followed by administration of IL-1 β . As GSK3 β activation was compromised in IL-1 β -treated AKT-KI^{+/+} mice, we tested whether hTau was phosphorylated at S199 in the cortex and hippocampus of AKT-KI^{-/-} and Akt-KI^{+/+} mice after administration of IL-1 β . We found that hTau phosphorylation was increased at S199 in the murine AKT-KI^{-/-} cortex and hippocampus after administration of IL-1 β . However, hTau phosphorylation at S199 was blocked in AKT-KI^{+/+} mice after administration of IL-1 β (Fig. 5A and B and *SI Appendix, Fig. S5E*). These results were further confirmed by confocal microscopic analysis, which showed that hTau S199 phosphorylation was decreased in the hippocampus (Fig. 5C and *SI Appendix, Fig. S5F*) and cortex (Fig. 5D and *SI Appendix, Fig. S5G*) of hTau-P301L-overexpressing IL-1 β -treated AKT-KI^{+/+} mice compared to hTau-P301L-overexpressing IL-1 β -treated AKT-KI^{-/-} mice. To further confirm these results, we isolated primary neurons

from AKT-KI^{+/+} mice overexpressing hTau-P301L, followed by IL-1 β treatment of the neurons. Next, we monitored hTau phosphorylation at S199. Consistent with our in vivo results, we found that the phosphorylation of hTau at S199 was blocked in AKT-KI^{+/+} neurons compared to AKT-KI^{-/-} neurons in association with an increase in GSK3 β phosphorylation (Fig. 5E and *SI Appendix, Fig. S5H*).

Since Tau phosphorylation at synapses significantly reduced the number of dendritic spines (43), we monitored the percentage of hTau-S199-P in the spines of neurons isolated from AKT-KI^{+/+} and AKT-KI^{-/-} mice. We found that the percentage of hTau-S199-P⁺ spines was decreased in IL-1 β -treated neurons isolated from AKT-KI^{+/+} mice (Fig. 5F and *SI Appendix, Fig. S5I*). The spine loss was further confirmed by monitoring the expression level of a postsynaptic protein, PSD95. We found that the reduced expression level of PSD95 in AKT-KI^{-/-} mice was rescued in AKT-KI^{+/+} mice after administration of IL-1 β (Fig. 5G and *SI Appendix, Fig. S5J*). The morphologic assessment of spines using DiI staining of AKT-KI^{+/+} mice revealed a loss of several spines in the cortex and hippocampus (Fig. 5H and I) that was rescued in AKT-KI^{+/+} mice after administration of IL-1 β . Similarly, the decrease in spine length in the hippocampus (Fig. 5H and J) of AKT-KI^{-/-} mice were restored in AKT-KI^{+/+} mice.

Accumulation of hTau-S199-P in spines leads to synaptic dysfunctions, which is the most common underlying mechanism of memory impairment in AD (44). We subjected both AKT-KI^{+/+} and AKT-KI^{-/-} mice overexpressing hTau-P301L to the Y-maze and Barnes maze tests to monitor spatial learning and memory functions after administration of IL-1 β . In the Barnes maze test, mice are placed in the middle of a large elevated circle, which has 19 mock holes and 1 target hole, and the time spent in the target quadrant is measured. The target quadrant is defined as the area containing the target hole and two more holes left and right side of the target hole. This is conducted for 4 training days. On the fifth day, the escape hole is blocked and the time spent in the target quadrant are measured. We found that the time spent in the target quadrant was increased for AKT-KI^{+/+}-overexpressing hTau-P301L treated with or without IL-1 β during the training period of 4 d (Fig. 5K). However, the time spent in the target quadrant was not improved in AKT-KI^{-/-}-overexpressing hTau-P301L mice treated with IL-1 β compared to untreated AKT-KI^{-/-} mice overexpressing hTau-P301L (Fig. 5K). On the day of the probe test, IL-1 β -treated AKT-KI^{+/+}-overexpressing hTau-P301L (Fig. 5L) mice spent more time in the target quadrant, compared to IL-1 β -treated AKT-KI^{-/-} mice overexpressing hTau-P301L (Fig. 5L). These data suggest that the memory function of AKT-KI^{-/-} mice overexpressing hTau-P301L was impaired after administration of IL-1 β . However, the memory function was rescued in AKT-KI^{+/+} mice under similar experimental conditions.

Consistent with the Barnes maze test, we found that the total number of triad alternations in the Y-maze was reduced significantly in hTau-P301L-overexpressing IL-1 β -treated AKT-KI^{-/-} mice compared to hTau-P301L-overexpressing IL-1 β -treated AKT-KI^{+/+} mice (Fig. 5O). This result suggests that AKT-KI^{+/+} mice attenuate cognitive dysfunction. However, the total number of arm entries (Fig. 5M) and total alternations (Fig. 1N) was altered between hTau-P301L-overexpressing IL-1 β -treated AKT-KI^{-/-} mice and hTau-P301L-overexpressing IL-1 β -treated AKT-KI^{+/+} mice. This indicates that there were no major differences in motor functions of AKT-KI^{+/+} and AKT-KI^{-/-} mice. Overall, our data suggest that blocking AKT sulphydration is essential to improving memory functions of mice overexpressing hTau-P301L under neuroinflammatory conditions.

In order to test whether the impairment of cognitive functions is also mediated by neuronal loss other than spine loss, we monitored neuronal loss as a characteristic feature of atrophy or neurodegeneration in hTau-P301L-overexpressing AKT-KI^{+/+} mice and AKT-KI^{-/-} mice. We found that overexpression of

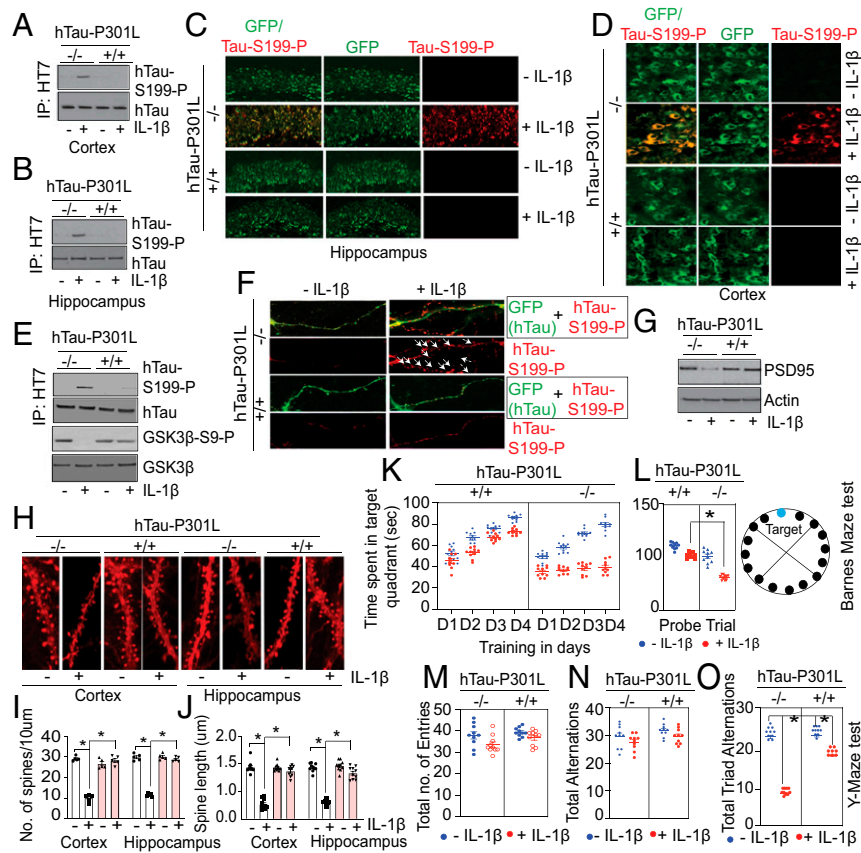


Fig. 5. In AKT-KI^{+/+} mice, the synaptic integrity and cognitive dysfunction were restored compared to AKT-KI^{-/-} mice after administration of IL-1 β . (A and B) Compared to AKT-KI^{-/-} mice, the induction of hTau-S199 phosphorylation was restored in the cortex (A) and hippocampus (B) of AKT-KI^{+/+} mice overexpressing hTau-P301L, after administration of IL-1 β (10 ng) in the cortex. (C and D) The confocal analysis shows that the hTau-S199 phosphorylation was decreased in the hippocampus (C) and cortex (D) of AKT-KI^{+/+} compared to AKT-KI^{-/-} mice overexpressing hTau-P301L after administration of IL-1 β . (E) Compared to AKT-KI^{-/-} neurons, the induction of hTau-S199 phosphorylation was restored in AKT-KI^{+/+} neurons overexpressed with hTau-P301L, after administration of IL-1 β (10 ng). (F) Confocal microscopic studies show that the level of hTau-S199 phosphorylation in spines was reduced in AKT-KI^{+/+} neurons overexpressed with hTau-P301L after administration of IL-1 β (10 ng). (G) Western blot analysis shows that PSD95 was decreased in AKT-KI^{-/-} mice but rescued in AKT-KI^{+/+} mice overexpressing hTau-P301L after administration of IL-1 β . (H) Confocal microscopic analysis shows that the loss of synaptic puncta as shown by Dil staining in the cortex and hippocampus was rescued in AKT-KI^{+/+} mice overexpressing hTau-P301L after administration of IL-1 β . (I and J) The loss in the number of spines per 10 μ m of dendrites (I) and loss in spine length (μ m) of dendrites (J), were rescued in the cortex and hippocampus of AKT-KI^{+/+} mice compared to AKT-KI^{-/-} mice after administration of IL-1 β . (K and L) The time spent in the target quadrant was improved IL-1 β -treated AKT-KI^{-/-} mice but rescued in AKT-KI^{+/+} mice overexpressing hTau-P301L compared to AKT-KI^{-/-} mice overexpressing hTau-P301L during 4 d of training (K) and the day of probe trial (L) in the Barnes maze test. A representative image of The Barnes maze was presented where the target hole was colored as blue while the other holes are shown in black color. (M–O) The total number of entries (M), total alternations (N), and the total number of triad alternations (O) were determined in the Y-maze test. The total number of entries, alternations was unaltered among AKT-KI^{+/+} mice or AKT-KI^{-/-} mice overexpressing hTau-P301L treated with or without IL-1 β . However, the total number of triad alternations was rescued in IL-1 β -treated AKT-KI^{+/+} mice overexpressing hTau-P301L compared to IL-1 β -treated AKT-KI^{-/-} mice overexpressing hTau-P301L. One-way ANOVA measured statistical significance with a Tukey–Kramer post hoc correction, $n = 10$, * $P < 0.05$. All data are expressed as mean \pm SEM. The arrowheads in F indicate the dendritic spines. (Magnification: C, 20 \times ; D, 40 \times ; F and H, 60 \times .)

hTau-P301L did not induce neuronal loss after a month of overexpression (SI Appendix, Fig. S5K). Our results are consistent with a previous study, which showed that PS19 mice developed neuronal loss and brain atrophy by 8 to 9 mo (37) despite cognitive impairment that was observed within 5 mo (45, 46).

Discussion

In the present study, we provide compelling evidence that AKT-P-SSH is critical for the activation of the protein kinase, GSK3 β , which in turn, augments the phosphorylation of hTau. Our study also reveals that the interaction between phosphorylated AKT and GSK3 β suppresses the activation of GSK3 β . Sulfhydration of phosphorylated AKT prevents the formation of the AKT–GSK3 β complex and the unbound unphosphorylated GSK3 β becomes free to phosphorylate Tau at S199 (SI Appendix, Fig. S5L). All of these events can be reversed in transgenic mice that block AKT sulfhydration.

The functional relevance of AKT in AD remains multifactorial (47, 48). Importantly, AKT plays a vital role in influencing the hyperphosphorylation of the microtubule-associated protein, Tau (49, 50), through GSK3 β phosphorylation. Inactivation of AKT has been shown to augment hTau hyperphosphorylation (50). However, the underlying mechanism for inactivation of AKT remains unknown. Previously, it was shown that in AD patient samples, phosphatase and tensin homolog deleted on chromosome 10 (PTEN) down-regulates the activation of AKT by decreasing its phosphorylation via inhibiting its localization to the plasma membrane (51–54). However, we show that sulfhydration of phosphorylated AKT (AKT-S473P-SSH or AKT-T308P-SSH) is the primary contributor to GSK3 β activation and it is possible that it functions independent of the PTEN-mediated reduction in AKT phosphorylation. In addition, the detection of AKT-P-SSH in AD patient samples and transgenic AD mice models, along with its correlation with hTau phosphorylation at S199, further

strengthens the evidence that AKT-S473P-SSH or AKT-T308P-SSH is critical in AD pathology.

Previously, dysregulation of H₂S homeostasis was implicated in the pathological processes of AD. Studies show that H₂S prevents neuronal impairment in an experimental model of AD (55). However, no studies have provided genetic evidence indicating whether a lack of H₂S exaggerated the neuropathology of AD. In addition, these studies were unable to provide direct evidence whether intracellular H₂S was down-regulated in AD. Our study contributes to these critical gaps in the field and establish that augmentation of H₂S plays an important role in the synaptic dysfunction in AD. In support of this conclusion, we provide compelling evidence using heterogeneous transgenic CBS mice and transgenic AKT-KI^{+/+} mice. As part of the mechanism, we found that AKT sulfhydrylation is critical for AD pathology, including Tau phosphorylation, which can be reversed in transgenic mice (AKT-KI^{+/+} mice) that block AKT sulfhydrylation. Sulfhydrylation of proteins is prevalent, and several proteins have been identified that are sulfhydrylated either under physiological or pathological conditions (34, 35, 56). Importantly, we found that AKT was not sulfhydrylated under physiological conditions. However, AKT can be sulfhydrylated under inflammatory conditions, which are present in all of the neurodegenerative disorders, including AD, Parkinson's disease, traumatic brain injury, and multiple sclerosis (57, 58). The investigation of the functional relevance of sulfhydrylated AKT in AKT-KI^{+/+} mice provides a unique opportunity to revisit the influence of AKT-P-SSH in the manifestation of these neurological disorders.

A substantial number of studies have shown that AKT is the major kinase that regulates the activation of GSK3 β . Other than AKT, the activation of other kinases, such as PKC or PKA, also contributes to the phosphorylation of GSK3 β at S9 (59, 60). Since GSK3 β phosphorylation is down-regulated in the AD brain, PKA or PKC may also play a role in the down-regulation of GSK3 β phosphorylation. GSK3 β phosphorylation is dependent on the intracellular H₂S levels, and the interaction between phosphorylated AKT and GSK3 β was robustly increased in the PS19 brain after depletion of H₂S. Thus, we mainly focused on the influence of AKT on GSK3 β phosphorylation. We provide direct evidence that blocking AKT sulfhydrylation in AKT-KI^{+/+} mice rescued GSK3 β phosphorylation. These data further confirm that AKT is the major kinase that regulates GSK3 β phosphorylation.

Previously, it was shown that Tau phosphorylation was independent of amyloid- β (A β) accumulation in the AD brain (61–63). However, the underlying mechanism was not fully elucidated. We provide evidence that proinflammatory cytokines can induce Tau phosphorylation before induction of A β in the AD brain (64, 65). On the other hand, A β and IL-1 β always function in a positive feedback loop. Thus, it is possible that induction of A β will further increase the sulfhydrylation of phosphorylated AKT and Tau phosphorylation through activation of GSK3 β in an IL-1 β -dependent manner.

Although the aggregation of hTau at the late phase of tauopathy has been associated with neuronal loss and brain atrophy (9–11), the early hyperphosphorylation of hTau, specifically at

S199, has a unique importance in synaptic dysfunction in AD patients. Aberrant hTau phosphorylation at the early stage of AD induces its mislocalization to dendritic spines and affects its stability (6–8). In addition, early phosphorylation of hTau serves as a precursor for hTau aggregation, which is a standard feature of tauopathy (62, 66). Thus, targeting early phosphorylation of hTau could be an effective strategy to reduce tauopathy. Our study provides direct evidence that sulfhydrylation of phosphorylated AKT is responsible for hTau hyperphosphorylation. In addition, we show that the loss of dendritic spines was rescued in AKT-KI^{+/+} mice, which resulted in an improvement in cognitive function. Thus, targeting sulfhydrylation of phosphorylated AKT provides a novel opportunity to address tauopathy in AD. In the future, we will study whether blocking AKT sulfhydrylation reduces brain atrophy and neuronal loss. Furthermore, tauopathy has been implicated in other neurological disorders other than AD (67). Thus, the identification of AKT sulfhydrylation may provide insights into other tauopathy-associated neurological disorders.

Materials and Methods

Animals. All mouse experiments were approved by the Institutional Animal Care and Use Committee of the University of Pittsburgh. The Akt-KI^{+/+} mouse colony was generated using the transgenic core facility of the University of Pittsburgh. The PS19 mouse line was purchased from the Jackson Laboratory. We used homozygous PS19^{+/+} males to carry out breeding with Akt-KI^{+/+} female mice to generate PS19^{+/+}:Akt-KI^{+/+} mice. The details of generation of AKT-KI^{+/+}, the maintenance and breeding of PS19 mice and PS19^{+/+}:Akt-KI^{+/+} mice are detailed in *S1 Appendix*. Details of materials and methods, including in vivo overexpression of mutant Tau construct and administration of IL-1 β in the brain, cortical neuron culture, site-specific mutagenesis, transfection in HEK293 cells and primary neurons, immunocytochemical and immunohistochemical staining, maleimide assay, coimmunoprecipitation, modified biotin switch assay for sulfhydrylation, quantitative real-time PCR, ELISA detection of hydrogen sulfide, agarose gel electrophoresis for the separation of DNA Western blotting, and neuro-behavioral tests like Y-maze test, Barnes maze test, open-field test, Dil stain, and spine evaluation are described in *S1 Appendix*. The quantification of each image present in the main figures is also incorporated in *S1 Appendix*.

Statistical Analysis. The biochemical studies, Western blot, coimmunoprecipitation, ELISA, RT-PCR, confocal analysis, the Sholl analysis, and all behavioral tests were statistically analyzed using one-way ANOVA and multiple comparisons were performed using the Tukey–Kramer post hoc test ($P < 0.05$) unless noted otherwise. Mean values were calculated for each biochemical experiment ($n = 7$) and each behavioral experiment ($n = 10$), and all of the data were depicted as the mean \pm SEM.

Data Availability. All data are available in the manuscript and *S1 Appendix*.

ACKNOWLEDGMENTS. We thank Dr. Sebastien Gingras (University of Pittsburgh School of Medicine, Department of Immunology) for the design of the targeting strategy; as well as Dr. Chunming Bi and Zhaohui Kou of the Transgenic and Gene Targeting Core (University of Pittsburgh School of Medicine, Department of Immunology) for the microinjection of zygotes and the production of mutant mice. This work was partly supported by National Institutes of Health Grants R01NS094516 and R01EY025622 (to N.S.) and by grants from the University of Pittsburgh and Copeland Foundation (to T.S. and N.S.).

1. C. A. Gold, A. E. Budson, Memory loss in Alzheimer's disease: Implications for development of therapeutics. *Expert Rev. Neurother.* **8**, 1879–1891 (2008).
2. R. Tarawneh, D. M. Holtzman, The clinical problem of symptomatic Alzheimer disease and mild cognitive impairment. *Cold Spring Harb. Perspect. Med.* **2**, a006148 (2012).
3. E. Tulving, Episodic memory: From mind to brain. *Annu. Rev. Psychol.* **53**, 1–25 (2002).
4. G. M. Shankar, D. M. Walsh, Alzheimer's disease: Synaptic dysfunction and Abeta. *Mol. Neurodegener.* **4**, 48 (2009).
5. J. Marsh, P. Alifragis, Synaptic dysfunction in Alzheimer's disease: The effects of amyloid beta on synaptic vesicle dynamics as a novel target for therapeutic intervention. *Neural Regen. Res.* **13**, 616–623 (2018).
6. C. A. Maurice, N. Sergeant, M. M. Ruchoux, J. J. Hauw, A. Delacourte, Phosphorylated serine 199 of microtubule-associated protein tau is a neuronal epitope abundantly expressed in youth and an early marker of tau pathology. *Acta Neuropathol.* **105**, 89–97 (2003).
7. J. Luna-Muñoz, L. Chávez-Macías, F. García-Sierra, R. Mena, Earliest stages of tau conformational changes are related to the appearance of a sequence of specific phospho-dependent tau epitopes in Alzheimer's disease. *J. Alzheimers Dis.* **12**, 365–375 (2007).
8. J. Bertrand, V. Plouffe, P. Sénéchal, N. Leclerc, The pattern of human tau phosphorylation is the result of priming and feedback events in primary hippocampal neurons. *Neuroscience* **168**, 323–334 (2010).
9. Z. Berger et al., Accumulation of pathological tau species and memory loss in a conditional model of tauopathy. *J. Neurosci.* **27**, 3650–3662 (2007).
10. Adel. C. Alonso, A. Mederlyova, M. Novak, I. Grundke-Iqbal, K. Iqbal, Promotion of hyperphosphorylation by frontotemporal dementia tau mutations. *J. Biol. Chem.* **279**, 34873–34881 (2004).
11. J. S. Song, S. D. Yang, Tau protein kinase I/GSK-3 beta/kinase FA in heparin phosphorylates tau on Ser199, Thr231, Ser235, Ser262, Ser369, and Ser400 sites phosphorylated in Alzheimer disease brain. *J. Protein Chem.* **14**, 95–105 (1995).

12. Z. Cai, Y. Zhao, B. Zhao, Roles of glycogen synthase kinase 3 in Alzheimer's disease. *Curr. Alzheimer Res.* **9**, 864–879 (2012).
13. C. X. Gong, K. Iqbal, Hyperphosphorylation of microtubule-associated protein tau: A promising therapeutic target for Alzheimer disease. *Curr. Med. Chem.* **15**, 2321–2328 (2008).
14. V. M. Lee, K. R. Brunden, M. Hutton, J. Q. Trojanowski, Developing therapeutic approaches to tau, selected kinases, and related neuronal protein targets. *Cold Spring Harb. Perspect. Med.* **1**, a006437 (2011).
15. J. Lim, K. P. Lu, Pinning down phosphorylated tau and tauopathies. *Biochim. Biophys. Acta* **1739**, 311–322 (2005).
16. T. Ma, GSK3 in Alzheimer's disease: Mind the isoforms. *J. Alzheimers Dis.* **39**, 707–710 (2014).
17. D. P. Hanger, W. Noble, Functional implications of glycogen synthase kinase-3-mediated tau phosphorylation. *Int. J. Alzheimers Dis.* **2011**, 352805 (2011).
18. A. Takashima, GSK-3 is essential in the pathogenesis of Alzheimer's disease. *J. Alzheimers Dis.* **9** (suppl. 3), 309–317 (2006).
19. K. Spittaels *et al.*, Glycogen synthase kinase-3beta phosphorylates protein tau and rescues the axonopathy in the central nervous system of human four-repeat tau transgenic mice. *J. Biol. Chem.* **275**, 41340–41349 (2000).
20. B. D. Manning, A. Toker, AKT/PKB signaling: Navigating the network. *Cell* **169**, 381–405 (2017).
21. A. Kremer, J. V. Louis, T. Jaworski, F. Van Leuven, GSK3 and Alzheimer's disease: Facts and fiction. *Front. Mol. Neurosci.* **4**, 17 (2011).
22. D. A. Cross, D. R. Alessi, P. Cohen, M. Andjelkovic, B. A. Hemmings, Inhibition of glycogen synthase kinase-3 by insulin mediated by protein kinase B. *Nature* **378**, 785–789 (1995).
23. D. R. Alessi, F. B. Caudwell, M. Andjelkovic, B. A. Hemmings, P. Cohen, Molecular basis for the substrate specificity of protein kinase B; comparison with MAPKAP kinase-1 and p70 S6 kinase. *FEBS Lett.* **399**, 333–338 (1996).
24. A. Ruckle *et al.*, Akt activity in Alzheimer's disease and other neurodegenerative disorders. *Neuroreport* **15**, 955–959 (2004).
25. J. J. Pei *et al.*, Role of protein kinase B in Alzheimer's neurofibrillary pathology. *Acta Neuropathol.* **105**, 381–392 (2003).
26. J. J. Pei *et al.*, Distribution of active glycogen synthase kinase 3beta (GSK-3beta) in brains staged for Alzheimer disease neurofibrillary changes. *J. Neuropathol. Exp. Neurol.* **58**, 1010–1019 (1999).
27. J. Avila *et al.*, Tau phosphorylation by GSK3 in different conditions. *Int. J. Alzheimers Dis.* **2012**, 578373 (2012).
28. C. Hooper, R. Killick, S. Lovestone, The GSK3 hypothesis of Alzheimer's disease. *J. Neurochem.* **104**, 1433–1439 (2008).
29. J. M. Rubio-Perez, J. M. Morillas-Ruiz, A review: Inflammatory process in Alzheimer's disease, role of cytokines. *ScientificWorldJournal* **2012**, 756357 (2012).
30. W. Swardfager *et al.*, A meta-analysis of cytokines in Alzheimer's disease. *Biol. Psychiatry* **68**, 930–941 (2010).
31. C. Liu, G. Cui, M. Zhu, X. Kang, H. Guo, Neuroinflammation in Alzheimer's disease: Chemokines produced by astrocytes and chemokine receptors. *Int. J. Clin. Exp. Pathol.* **7**, 8342–8355 (2014).
32. F. Brosseon, M. Krauthausen, M. Kummer, M. T. Heneka, Body fluid cytokine levels in mild cognitive impairment and Alzheimer's disease: A comparative overview. *Mol. Neurobiol.* **50**, 534–544 (2014).
33. A. Kimura, N. Yoshikura, Y. Hayashi, T. Inuzuka, Cerebrospinal fluid C-C motif chemokine ligand 2 correlates with brain atrophy and cognitive impairment in Alzheimer's disease. *J. Alzheimers Dis.* **61**, 581–588 (2018).
34. S. Mir, T. Sen, N. Sen, Cytokine-induced GAPDH sulfhydrylation affects PSD95 degradation and memory. *Mol. Cell* **56**, 786–795 (2014).
35. B. D. Paul, S. H. Snyder, H₂S signalling through protein sulfhydrylation and beyond. *Nat. Rev. Mol. Cell Biol.* **13**, 499–507 (2012).
36. A. K. Mustafa *et al.*, H₂S signals through protein S-sulfhydrylation. *Sci. Signal.* **2**, ra72 (2009).
37. Y. Yoshiyama *et al.*, Synapse loss and microglial activation precede tangles in a P301S tauopathy mouse model. *Neuron* **53**, 337–351 (2007).
38. K. E. Hopperton, D. Mohammad, M. O. Trépanier, V. Giuliano, R. P. Bazinet, Markers of microglia in post-mortem brain samples from patients with Alzheimer's disease: A systematic review. *Mol. Psychiatry* **23**, 177–198 (2018).
39. X. Liu, N. Quan, Microglia and CNS interleukin-1: Beyond immunological concepts. *Front. Neurol.* **9**, 8 (2018).
40. L. C. Cantley, The phosphoinositide 3-kinase pathway. *Science* **296**, 1655–1657 (2002).
41. I. Vivanco, C. L. Sawyers, The phosphatidylinositol 3-kinase AKT pathway in human cancer. *Nat. Rev. Cancer* **2**, 489–501 (2002).
42. S. Yang *et al.*, Reducing the levels of Akt activation by PDK1 knock-in mutation protects neuronal cultures against synthetic amyloid-beta peptides. *Front. Aging Neurosci.* **9**, 435 (2018).
43. R. Kandimalla, M. Manczak, X. Yin, R. Wang, P. H. Reddy, Hippocampal phosphorylated tau induced cognitive decline, dendritic spine loss and mitochondrial abnormalities in a mouse model of Alzheimer's disease. *Hum. Mol. Genet.* **27**, 30–40 (2018).
44. J. Di *et al.*, Abnormal tau induces cognitive impairment through two different mechanisms: Synaptic dysfunction and neuronal loss. *Sci. Rep.* **6**, 20833 (2016).
45. H. Takeuchi *et al.*, P301S mutant human tau transgenic mice manifest early symptoms of human tauopathies with dementia and altered sensorimotor gating. *PLoS One* **6**, e21050 (2011).
46. C. A. Lasagna-Reeves *et al.*, Reduction of Nuak1 decreases tau and reverses phenotypes in a tauopathy mouse model. *Neuron* **92**, 407–418 (2016).
47. R. J. Griffin *et al.*, Activation of Akt/PKB, increased phosphorylation of Akt substrates and loss and altered distribution of Akt and PTEN are features of Alzheimer's disease pathology. *J. Neurochem.* **93**, 105–117 (2005).
48. A. Sanabria-Castro, I. Alvarado-Echeverría, C. Monge-Bonilla, Molecular pathogenesis of Alzheimer's disease: An update. *Ann. Neurosci.* **24**, 46–54 (2017).
49. C. Li, J. Götz, Tau-based therapies in neurodegeneration: Opportunities and challenges. *Nat. Rev. Drug Discov.* **16**, 863–883 (2017).
50. W. H. Stoothoff, G. V. Johnson, Tau phosphorylation: Physiological and pathological consequences. *Biochim. Biophys. Acta* **1739**, 280–297 (2005).
51. M. M. Georgescu, PTEN tumor suppressor network in PI3K-Akt pathway control. *Genes Cancer* **1**, 1170–1177 (2010).
52. S. Frere, I. Slutsky, Targeting PTEN interactions for Alzheimer's disease. *Nat. Neurosci.* **19**, 416–418 (2016).
53. S. Knafo *et al.*, PTEN recruitment controls synaptic and cognitive function in Alzheimer's models. *Nat. Neurosci.* **19**, 443–453 (2016).
54. P. Kreis, G. Leondaritis, I. Lieberam, B. J. Eickholt, Subcellular targeting and dynamic regulation of PTEN: Implications for neuronal cells and neurological disorders. *Front. Mol. Neurosci.* **7**, 23 (2014).
55. H. J. Wei, X. Li, X. Q. Tang, Therapeutic benefits of H₂S in Alzheimer's disease. *J. Clin. Neurosci.* **21**, 1665–1669 (2014).
56. N. Sen, Functional and molecular insights of hydrogen sulfide signaling and protein sulfhydrylation. *J. Mol. Biol.* **429**, 543–561 (2017).
57. G. Gelders, V. Baekelandt, A. Van der Perren, Linking neuroinflammation and neurodegeneration in Parkinson's disease. *J. Immunol. Res.* **2018**, 4784268 (2018).
58. R. M. Ransohoff, How neuroinflammation contributes to neurodegeneration. *Science* **353**, 777–783 (2016).
59. O. Kaidanovich-Beilin, J. R. Woodgett, GSK-3: Functional insights from cell biology and animal models. *Front. Mol. Neurosci.* **4**, 40 (2011).
60. X. Fang *et al.*, Phosphorylation and inactivation of glycogen synthase kinase 3 by protein kinase A. *Proc. Natl. Acad. Sci. U.S.A.* **97**, 11960–11965 (2000).
61. F. Kametani, M. Hasegawa, Reconsideration of amyloid hypothesis and tau hypothesis in Alzheimer's disease. *Front. Neurosci.* **12**, 25 (2018).
62. P. Saha, N. Sen, Tauopathy: A common mechanism for neurodegeneration and brain aging. *Mech. Ageing Dev.* **178**, 72–79 (2019).
63. R. Rajmohan, P. H. Reddy, Amyloid-beta and phosphorylated tau accumulations cause abnormalities at synapses of Alzheimer's disease neurons. *J. Alzheimers Dis.* **57**, 975–999 (2017).
64. J. W. Kinney *et al.*, Inflammation as a central mechanism in Alzheimer's disease. *Alzheimers Dement. (N. Y.)* **4**, 575–590 (2018).
65. F. Alasmari, M. A. Alshammari, A. F. Alasmari, W. A. Alanazi, K. Alhazzani, Neuroinflammatory cytokines induce amyloid beta neurotoxicity through modulating amyloid precursor protein levels/metabolism. *BioMed Res. Int.* **2018**, 3087475 (2018).
66. M. Kolarova, F. Garcia-Sierra, A. Bartos, J. Ríchny, D. Ripova, Structure and pathology of tau protein in Alzheimer disease. *Int. J. Alzheimers Dis.* **2012**, 731526 (2012).
67. V. M. Lee, M. Goedert, J. Q. Trojanowski, Neurodegenerative tauopathies. *Annu. Rev. Neurosci.* **24**, 1121–1159 (2001).